Progress in Superconductivity Vol.11 No.2 pp.141-146 30 April 2010

Phase Stability of Laser-ablated $SmBa_2Cu_3O_{7-y}$ thin Films Investigated by Raman Scattering Spectroscopy

G. Kim[a], A. R. Jeong[a], W. Jo[*,a], D. Y. Park[b], H. Cheong[b],
A. Tsukada[c], R. H. Hammond[c], and M. R. Beasley[c]

[a] *Department of Physics, Ewha Womans University, Seoul 120-750, Korea*

[b] *Department of Physics, Sogang University, Seoul 121-742, Korea*

[c] *Geballe Laboratory for Advanced Materials, Stanford University, Stanford, CA 94305, USA*

(Received 9 March 2010 revised or reviewed 30 March 2010 accepted 5 April 2010)

Abstract

Phase stability diagram and boundary of *a*- and *c*-axis orientation of $SmBa_2Cu_3O_{7-y}$ (SmBCO) thin films grown by pulsed laser deposition (PLD) were reported with studies based on x-ray diffraction [1]. Four different samples are systematically analyzed: normal *c*-axis oriented orthorhombic $SmBa_2Cu_3O_{7-y}$, *a*-axis oriented $SmBa_2Cu_3O_{7-y}$, *c*-axis oriented orthorhombic $SmBa_2Cu_3O_{7-y}$ with Sm_2BaCuO_5 phase, and a mixture with *c*-axis oriented orthorhombic $SmBa_2Cu_3O_{7-y}$ and anomalously long-*c* tetragonal $SmBa_2Cu_3O_x$. Raman scattering spectroscopy equipped with polarization analysis elucidates the crystal orientation and the origin of the growth of the materials. It indicates that the technique can be used for quality control of conductor manufacturing processes as well as for enhancement of the materials properties.

Keywords : SmBCO thin films, Raman scattering spectroscopy, and phase stability

I. Introduction

Rare-earth based cuprate (ReBCO) superconductors have been regarded as materials for coated-conductor applications since they show good pinning performance in high magnetic fields [2, 3]. Pulsed-laser deposition (PLD) [4], metal-organic deposition (MOD) [5], and co-evaporation with dual chambers are used as reproducible growth methods for the materials as the form of films are being developed [6]. The SmBCO superconducting materials have higher critical temperature and irreversible field than YBCO [7]. In previous work of Cai *et al.* [8], they fabricated high quality SmBCO by top-seeded solution (TSS) growth in 1 atm oxygen pressure. This single crystal shows T_c ~ 95 K and a sharp transition without secondary phases. Recently, Yoshida *et al.* reported that the critical current density of $SmBa_2Cu_3O_{7-y}$ (SmBCO) films at high magnetic fields can be enhanced by addition of nanostructured materials into the superconducting phase [9-11]. In this study, we investigate systematically four representative samples: normal *c*-axis oriented orthorhombic $SmBa_2Cu_3O_{7-y}$, *a*-axis oriented $SmBa_2Cu_3O_{7-y}$, *c*-axis oriented orthorhombic $SmBa_2Cu_3O_{7-y}$ with Sm_2BaCuO_5 phase, and a mixture with *c*-axis oriented orthorhombic $SmBa_2Cu_3O_{7-y}$ and anomalously long-*c* tetragonal $SmBa_2Cu_3O_x$. The properties of the materials in terms of crystalline orientation, phase, and orthorhombiciy vs. tetragonality have been studied in detail by x-ray diffraction (XRD) [1]. The morphology and the phonon modes at a small length scale should

*Corresponding author: William Jo
Tel : +82-2-3277-2322, Fax : +82-2-3277-4066
e-mail : wmjo@ewha.ac.kr

be addressed because the information is relevant in judging the growth mechanism and the nature of the two different materials. For this purpose, a combined study with scanning electron microscopy (SEM) is useful because the techniques are complementary for looking at the surface. Raman scattering spectroscopy is a powerful method to characterize and understand high- T_c materials [12]. The formation of $BaCu_2O_2$ second phases leads to peculiar vibrational modes in the Raman spectra, so that it is possible to trace back the processing records.

II. Experiments

The SmBCO films were deposited on (001) $LaAlO_3$ substrates by PLD over a wide range of oxygen partial pressure and substrate temperature. In particular, we focus on the growth at low oxygen pressure since SmBCO is known to have anti-site disorder when it is grown at high oxygen pressure conditions [13]. XRD showed a very clean "*c*" axis, i.e., no "*a*" or other phases, but had two "*c*" lattices. As described in previous reports, off axis diffraction revealed: a nominal orthorhombic lattice with a nominal "*a*", "*b*", and "*c*" lattice constants and an anomalous tetragonal lattice with a 1 % larger lattice constant [1].

Figure 1 displays that the partial oxygen pressure (PO_2) versus substrate temperature (*Ts*) diagram indicating the growth conditions of the four SmBCO films. It shows the YBCO stability region (solid lines) and the SmBCO stability line as found in the *in-situ* PLD investigation (the red line) [1]. Firstly, sample (*A*) grown at 900 °C with 400 mTorr pure O_2 gas has a normal *c*-axis superconductivity phase. This sample was cooled down in O_2 gas with 400 mTorr, and then cooled again in a tube furnace until 350 °C with flowing O_2 gas at 100 sccm for 1 hour. The second sample (*B*) was made at a low substrate temperature to be compared with other samples. It was grown with the *a*-axis orientation. The third sample (*C*) was an as-grown sample which was treated with O_2 and Ar annealing. It has a mixture of the normal superconducting phase and a secondary Sm_2BaCuO_5 (211) phase. Sample (*D*) seems to have a normal c-axis superconductivity phase. It has, however, two lattice parameters with c-axis oriented orthorhombic $SmBa_2Cu_3O_{7-y}$ and anomalously long-c tetragonal $SmBa_2Cu_3O_x$ phases. This film (*D*) was cooled at 200 mTorr in O_2. The details of the sample preparation and characterization are described in Ref. [1]. The thickness of the samples is 500 nm.

In this study, the four samples were characterized by XRD, SEM and Raman scattering spectroscopy. SEM was measured with a field emission scanning electron microscope (JEOL, JSM-6330F). The Raman scattering spectra were measured in a quasi-backscattering geometry using 40 mW of the 514.5 nm wavelength of an Ar ion laser. In the polarization combinations of the incident and scattered light are denoted as XX, XY, YX and YY. Here, XY, for example, represents the incident light polarization in the horizontal direction and the scattered light polarization in the vertical direction.

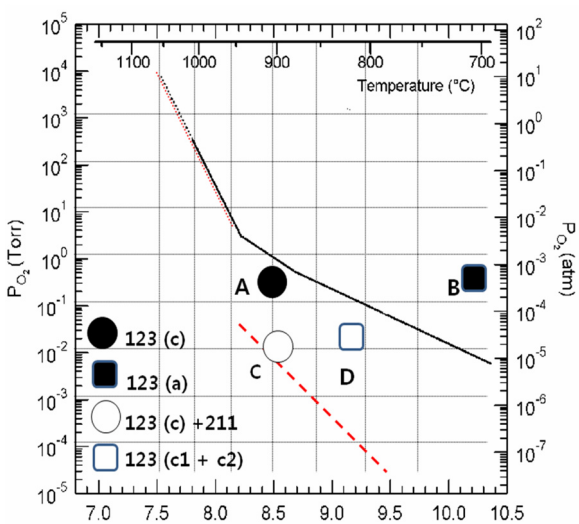

Fig. 1. Phase stability diagram of PLD in-situ growth of SmBCO. The growth conditions for the four samples studied are indicated.

III. Results and discussion

Figure 2 shows XRD θ-2θ patterns of the four

SmBCO films. SmBCO (00*l*) reflections and secondary phase peaks of the 211 phase are identified from the patterns.

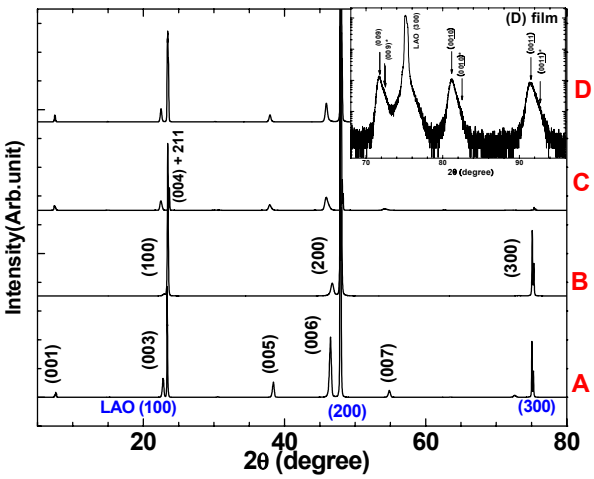

Fig. 2. X-ray diffraction pattern (XRD) of SmBCO (a) *A*: well grown with the c-axis orientation (b) *B*: grown with the a-axis orientation (c) *C*: grown with the c-axis orientation and secondary phase (Sm211) (d) *D*: grown with the c-axis orientation (2 lattice parameters).

In the pattern of the (*A*) film, it clearly shows SmBCO (00*l*) and $LaAlO_3$ (*h*00) layers indicating that the samples have a *c*-axis orientation with no impurity phases. In addition, we cannot observe any secondary peaks such as 211 or $BaCu_2O_2$. It means that the film was grown with *c*-axis orientation normal to the surface. The diffraction pattern of sample (*B*) is quite different from those of the other samples. The spectrum shows the *a*-axis peaks which overlapped with substrate peaks. The crystal growth behaviors of this sample will be clearly addressed by Raman scattering spectroscopy. In the cases of samples (*C*) and (*D*), the diffraction patterns are basically similar to that of sample (*A*). However, the diffraction pattern of sample (*C*) has secondary Sm_2BaCuO_5 peaks which appeared near the (004) peak. Sample (*D*) has different lattice parameters: *c*-axis oriented orthorhombic $SmBa_2Cu_3O_{7-y}$ and anomalously long-*c* tetragonal $SmBa_2Cu_3O_x$. The peaks marked with asterisks of (009) and (00$\underline{11}$) show clear separation of the *c*-axis peaks for longer *c*-axis grains and shorter *c*-axis grains, even though they have small intensities. From these results, we can confirm the crystal orientation of the films, secondary phases, and longer *c*-axis and shorter *c*-axis, and orthorhombic vs. tetragonal symmetry as compared with the phase diagram.

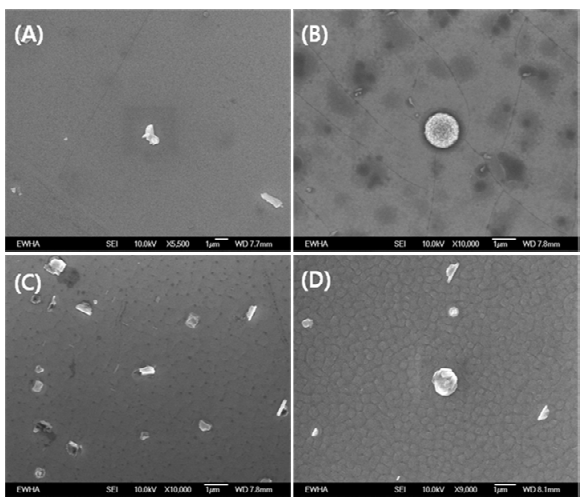

Fig. 3. Scanning electronic microscopy (SEM) images of (a) *A*: folded grain (b) *B*: cracks around bud (~1500 nm) and black spots (c) *C*: many grains and holes on the surface (d) *D*: many grains all over the surface of the film.

Figure 3 shows SEM images of the SmBCO samples. The spatial scale of each SEM image is denoted in each figure. The image of film (*A*) looks mostly homogeneous, and but some significant features are observed on the surface, which may originate from the liquid-phase [14]. The film (*B*), which was characterized as *a*-axis oriented however, has black spots on the surface and buds with cracks around it. The film (*C*), which was grown as *c*-axis oriented with second phase 211, has many grains and holes on the surface with 500~1000 nm grain sizes. In particular, we can observe parallel white lines on the surface indicating the axes of the film. In the image of sample (*D*), there are many grains over the surface with 1 micron size.

Figure 4 shows polarized Raman scattering spectra of the four SmBCO films taken at room temperature.

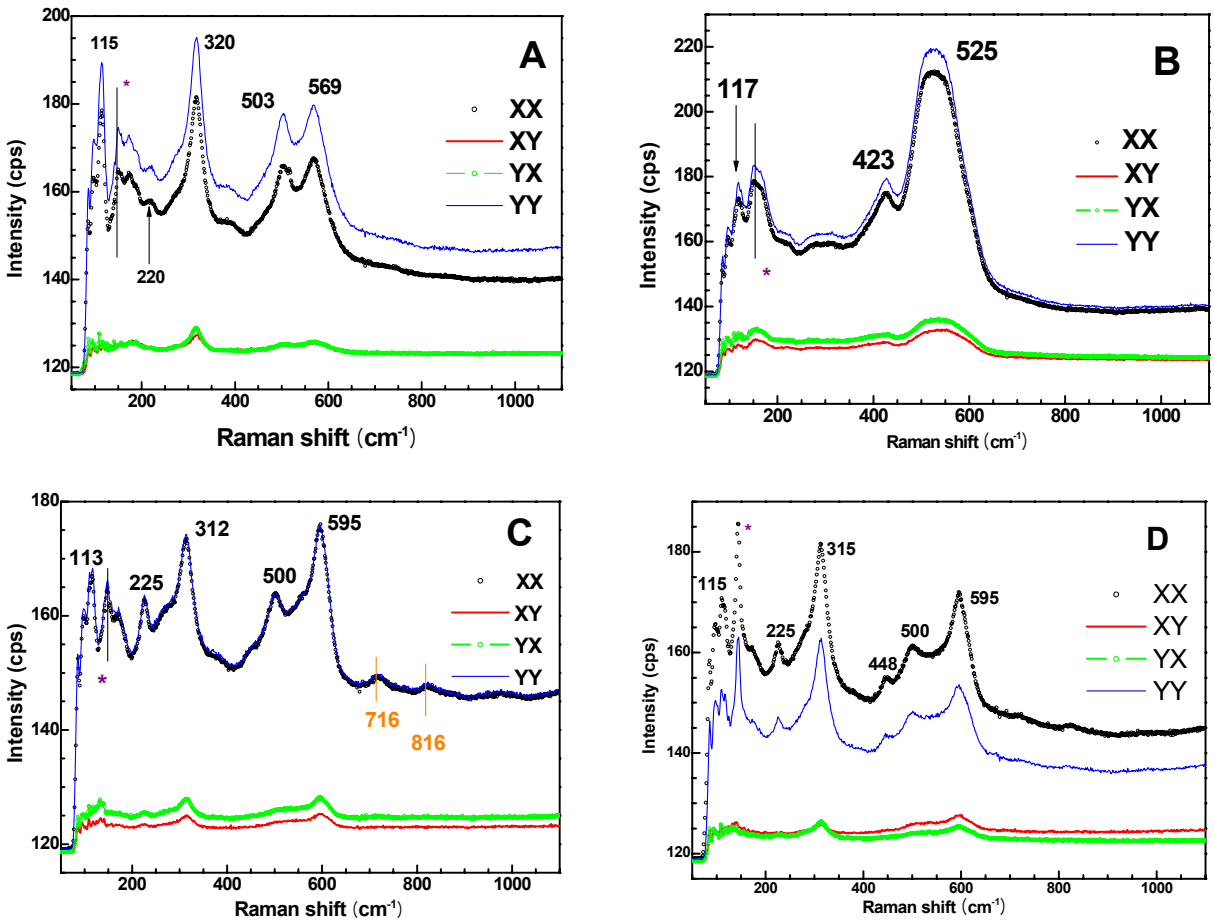

Fig. 4. Polarized Raman scattering spectra of the four SmBCO samples. The peak indicated with (*) is an experimental artifact.

We can observe Raman-active if the polarizability is changed during the vibration. Therefore, the spectra in the same sample have a different shape as an incident-light polarization and scattered light polarization. The long-pass edge filter used to remove the laser light has a cut-off at around 100 cm^{-1}, but it adds an artifact at 150 cm^{-1}, which appears as a peak in the spectra and indicated with an (*). The Raman spectra of the samples (*A*), (*C*) and (*D*) have peaks at around 115, 315, 448 and 500 cm^{-1}. It is revealed that the films at least consist of well-grown as *c*-axis oriented SmBCO phase. The spectra for sample (*B*) are significantly different as this sample is *a*-axis oriented.

The peak at 115 cm^{-1} is due to a Ba-Ba stretching mode. A Cu-Cu stretching mode in the CuO_2 plane is expected at around 145 cm^{-1} but is obscured by the peak (*) due to a system artifact. The peak near 315 cm^{-1} is ascribed to an out-of-phase O(2)+/O(3)- mode in the CuO_2 plane. This peak is not allowed in the a-axis oriented sample (*B*). The other two A_{1g} modes at 448 cm^{-1} and 500 cm^{-1} are the in-phase O(2)+/O(3)+ mode in the CuO_2 plane and the apical O(4) mode, respectively. In the spectra of sample (*B*), a broad peak centered around 525 cm^{-1} appears. This peak is probably a convolution of several peaks in this frequency range that appear in this scattering geometry. Several groups reported that the 500 cm^{-1}

band is sensitive to the oxygen content for YBCO. Hong *et al*. reported that the YBCO peak near 500 cm^{-1} is shifted by +25 cm^{-1} when it is treated in oxygen deficient ambient [15]. In addition, the peak around 600 cm^{-1} is also dependent on the oxygen vacancy. Therefore, it is reasonable to suppose that the 500 cm^{-1} band may be closely related with the oxygen content [16]. The 503 cm^{-1} Raman peak, which is due to the O-O stretching of the apical oxygen along the *z*-axis, is softened when O concentration decreases and tends to appear around 500 ± 5 cm^{-1}. However, the peak near 570 cm^{-1} which is due to another O-O stretching mode, is shifted depending on the growth conditions. On the other hand, the sample (*C*) shows extra peaks above 700 cm^{-1} which are related to the 211 phase. Rosen *et al.* [17] found that even small concentration of impurity phases in the YBCO samples can strongly influence the Raman spectra.

IV. Summary

Growth of SmBCO films with high quality is a challenging task, requiring fine tuning of growth conditions such as the substrate temperature and the partial oxygen pressure. Second phases such as the 211 phase can be easily confirmed by Raman scattering spectroscopy, whereas other possible liquid phases like $BaCu_2O_2$ are not observed in our SmBCO samples since the growth temperature is much lower than YBCO or NdBCO. Morphological studies give us some clues on the growth mechanism and the possibility of pinning centers. From this study, we can obtain a possible route of optimal growth conditions for SmBCO coated conductors, and furthermore, important basis for Raman analysis of a variety of materials involved, which is critical for quality control during HTS manufacturing processes.

Acknowledgments

This research was supported by a grant from Center for Applied Superconductivity Technology of the 21st Century Frontier R&D Program funded by the Ministry of Education, Science and Technology, Republic of Korea. The work at Sogang University was supported by Basic Science Research Program through the National Research Foundation of Korea (NRF) grant funded by the MEST (No. R01-2008-000-10685-0).

References

[1] A. Tsukada, I. G. Chen, R. H. Hammond, and M. R. Beasley, *IEEE Transactions on Applied Superconductivity* **19**, 3383 (2009).

[2] M. Murakami, S. I. Yoo, T. Higuchi, N. Sakai, M. Watabiki, N. Koshizuka, and S. Tanaka, *Physica* C **463-235**, 2781 (1994).

[3] S. I. Yoo, M. Murakami, N. Sakai, T. Ohyama, T. Higuchi, M. Watahiki, and M Takahashi *J. Electron. Mater.* **24**, 1923 (1995).

[4] S. Funaki, Y. Yoshida, Y. Ichino, M. Miura, Y. Takai, K. Matsumoto, A. Ichinose, M. Mukaida, and S. Horii, *Physica* C **463-465**, 644 (2007).

[5] G.-M Shin, D.-J. Kim, K.-J. Song, C. Park, S.-H. Moon, and S. I. Yoo, *IEEE Transactions on Applied Superconductivity* **17**, 3561 (2007).

[6] B. S. Lee, K. C. Chung, S. M. Lim, H. J. Kim, D. Youm, and C. Park, *Supercond. Sci. Technol.* **17**, 580 (2004).

[7] K. Shdoh, Y. Ichino, Y. Yoshida, Y. Takai, and I. Hirabayashi, *IEEE Transactions on Applied Superconductivity* **12**, 2795 (2003).

[8] Y. Q. Cai, X. Yao, A. Hu, X. J. Wu, M. Jirsa, S. Xu, and G. Jin, *Supercond. Sci. Technol*. **19**, S506 (2006).

[9] M. Miura, Y. Yoshida, Y. Ichino, Y. Takai, K. Matsumoto, A. Ichinose, S. Horii, and M. Mukaida *Japan. J. Appl. Phys*. **45**, L11(2006).

[10] Y. Yoshida, K. Matsumoto, M. Miura, Y. Ichino, Y. Takai, A. Ichinose, M. Mukaida, and S Horii *Physica* C **445-448**, 637 (2006).

[11] M. Miura, Y. Ichino, Y. Yoshida, Y. Takai, K. Matsumoto, A. Ichinose, S. Horii, and M. Mukaida, *Physica* C **445-448**, 643 (2006).

[12] G. A. Kourouklis, A. Jayaraman, B. Batlogg, R. J. Cava, M. Stavola, D. M. Krol, E. A. Rietman, and L. F. Schneemeyer, *Phys. Rev.* B **36**, 8320 (1987).
[13] X. Yao, X. H. Zeng, S. Xu, *Physica* C **412-414**, 90 (2004).
[14] T. Ohnishi, J.-U. Huh, R. H. Hammond, and W. Jo, *J. Mater. Res*. **19**, 977 (2004).
[15] S. S. Hong, K. M. Kim, H. S. Cheong, and G. S. Park, *Physica* C **454**, 82 (2007).
[16] M. Hangyo, S. Nakashima, N. Hasegawa, S. Hayashi, and K. Wasa, *Japan. J. Appl. Phys*. **29**, 851 (1990).
[17] H. J. Rosen, R. M. Macfarlane, E. M. Engler, V. Y. Lee, and R. D. Jacowitz, *Phys. Rev*. B **38**, 2460 (1988).